Available online at www.sciencedirect.com
ScienceDirect
Trans. Nonferrous Met. Soc. China 20(2010) 2174−2180
Transactions of Nonferrous Metals Society of China
www.tnmsc.cn

Cyclic deformation behaviors of Ti-46Al-2Cr-2Nb-0.15B alloy during thermo-mechanical fatigue tests

XIANG Hong-fu(项宏福)[1], DAI An-lun(戴安伦)[1], WANG Ji-heng(王冀恒)[1], LI Hui(李 惠)[1], YANG Rui(杨 锐)[2]

1. Provincial Key Laboratory of Advanced Welding Technology, Jiangsu University of Science and Technology, Zhenjiang 212003, China;
2. Institute of Metal Research, Chinese Academy of Sciences, Shenyang 110016, China

Received 23 October 2009; accepted 15 August 2010

Abstract: Thermo-mechanical fatigue tests were carried out on the gamma-TiAl alloy in the temperature range of 500−800 °C under mechanical strain control in order to evaluate its cyclic deformation behaviors at elevated temperature. Cyclic deformation curves, stress−strain hysteresis loops under different temperature−strain cycles were analyzed and dislocation configurations were also observed by TEM. The mechanisms of cyclic hardening or softening during thermo-mechanical fatigue (TMF) tests were also discussed. Results showed that thermo-mechanical fatigue lives largely depended on the applied mechanical strain amplitudes, applied types of strain and temperature. On the hysteresis loops appeared two apparent asymmetries: one was zero asymmetry and the other was tensile and compressive asymmetry. Dislocations configuration and slip behaviors were contributed to cyclic hardening or cyclic softening.

Key words: titanium-aluminium alloy; thermo-mechanical fatigue; cyclic stress response; hysteresis loop; dislocation

1 Introduction

Near-γ titanium aluminides are currently receiving much attention as candidates for high temperature structural application in aerospace and automobile industries because of their low density, high strength and stiffness at high temperature, and excellent creep and oxidation resistance[1−4].

In recent years, most work has been focused on the optimization of composition and thermo-mechanical pre-treatment in order to improve ductility and fracture toughness. And oxidation, creep and fatigue crack growth behaviors at various temperatures were also dealt with in numerous studies[5−10]. However, little information exists on the high temperature cyclic stress−strain (CSR) behaviors, and results from thermo-mechanical fatigue (TMF) tests about titanium aluminium alloys have been a little reported as to the authors' knowledge[11−18].

Recent researches showed that fatigue behavior was found to be strongly affected by temperature as a consequence of a change in the cyclic stress–strain response at about 650 °C. At temperatures lower than 650 °C, initial cyclic hardening occurred, whereas above 650 °C a cyclic saturation state was observed from the beginning[11]. OP (out-of-phase) loading led to high positive and IP (in-phase) loading to high negative mean stresses[12]. The fatigue lives were well described by the Smith-Watson-Topper damage parameter[11, 17]. In the present work, cyclic deformation behaviors of as-cast Ti-46Al-2Cr-2Nb-0.15B alloy during thermo-mechanical fatigue tests are explored. Thus, we can acquire its deformation behaviors, fatigue endurance and resistance to oxidation at elavated temperature as important high temperature structural applications in aerospace and automobile industries.

2 Experimental

The nominal compositions of Ti-46Al-2Cr-2Nb-0.15B are shown in Table 1. Ingots were prepared by centrifugal casting after consumable electrode melting, hot isostatically pressed (HIPed) at 1 280 °C and 200 MPa for 4 h followed by heat treatment at 900 °C for 4 h. As can be seen in Fig.1, microstructure of this alloy consisted of α_2/γ colonies and some borides distributed along grain boundaries and phase interfaces. Tensile

Foundation item: Project(SBK200930307) supported by Natural Science Foundation of Jiangsu Province, China
Corresponding author: XIANG Hong-fu; Tel: +86-511-84401188; E-mail: hfxiangimr@yahoo.com.cn
DOI: 10.1016/S1003-6326(09)60438-6

properties of this alloy are shown in Fig.2. Tensile strength decreased little till 650 °C, but above 650 °C it descended rapidly; while elongation and reduction of area enhanced largely with temperature increasing. Yield strength continuously declined with temperature increasing. Strain rate almost had no effect on yield strength, but tensile strength, elongation and reduction of area had a drop evidently when strain rate rose from 1.74×10^{-4} s^{-1} to 3.74×10^{-4} s^{-1}, and it was surprisingly seen that strength and plasticity showed no change with the increase of strain rate from 3.74×10^{-4} s^{-1} to 1.74×10^{-3} s^{-1}.

Table 1 Nominal composition of Ti-46Al-2Cr-2Nb-0.15B alloy (molar fraction, %)

Al	Cr	Nb	B	Ti
43.663 3	2.112 4	2.085 3	0.15	Bal.

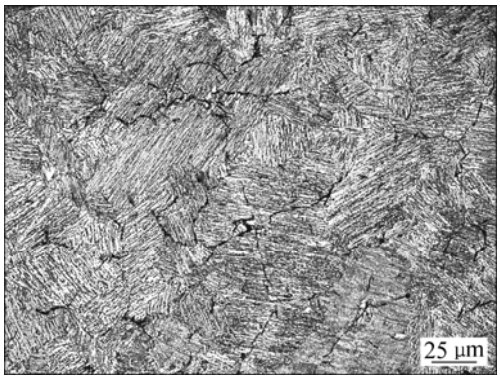

Fig.1 Microstructure of near gamma-TiAl before TMF tests

TMF tests were carried out on a servo-hydraulic testing system MTS810 under mechanical strain control using a triangle wave-shape on smooth cylindrical specimens with a gauge length of 18 mm and a diameter of 7 mm. The specimens were heated with a high frequency induction heater. Heating rate was 5 K/s and axial temperature deviations within the gauge length were in ±5 °C.

Temperature was measured with a thermocouple fixed on specimen by a spot-welder. All tests were performed in laboratory. Two different TMF temperature−strain cycles such as in-phase (IP) and out-of-phase (OP) were performed. The test temperature range (500−800 °C) were used during in-phase (IP) and out-of-phase (OP) TMF tests with 500 °C and 800 °C as the minimum and maximum temperature, respectively. Mechanical strain amplitude ranged from 0.20% to 0.85%. Strain rate of TMF tests was confined to 6.67×10^{-5} s^{-1}.

The mechanical strain ε_{mech} was calculated from the total measured strain ε_{total} by subtraction of the thermal expansion strain ε_{ther}:

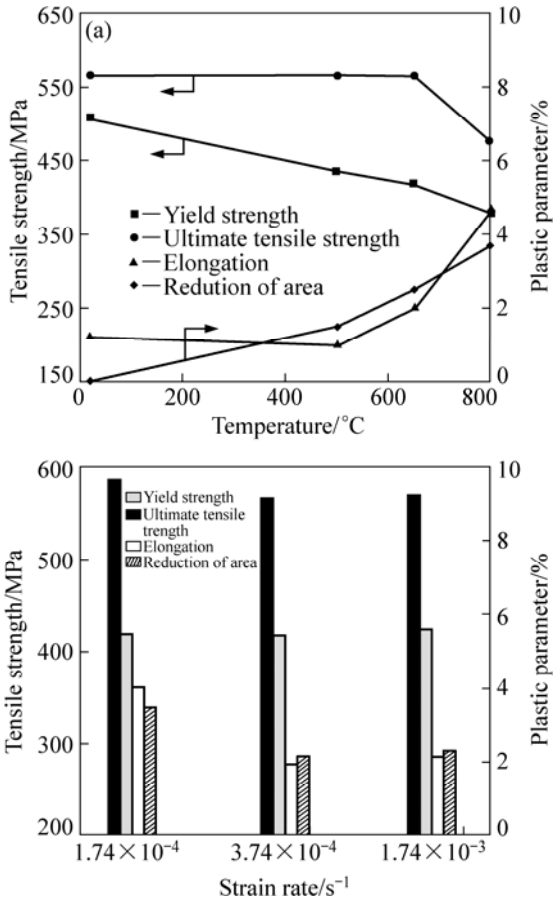

Fig.2 Tensile properties of Ti-46Al-2Cr-2Nb-0.15B alloy: (a) Temperature-dependent; (b) Strain rate-dependent

$$\Delta\varepsilon_{mech} = \Delta\varepsilon_{total} - \Delta\varepsilon_{ther} \quad (1)$$

For an exact strain measurement, the testing system has to be in thermally steady state. Therefore, four initial cycles at zero stress were carried out before determination of thermal expansion, thermal expansion strain compensation and testing.

Subsequently, two initial heating cycles were carried out on all samples before the first TMF test. In the first cycle, a stress-controlled test at zero stress was used in order to determine the thermal expansion of the samples. The second cycle was carried out in mechanical strain control with zero mechanical strain as control value (i.e. totally measured strain minus thermal strain). In the second cycle, the stress was less than 20 MPa at all points of the hysteresis loops, which showed that the thermal expansion strain compensation worked correctly.

The microstructural details and dislocation arrangements were studied after testing by transmission electron microscopy (TEM) using a Philips CM 30. The samples were prepared by electrolytic double jet thinning at a temperature of −30 °C with a methanol-butanol perchloric acid electrolyte.

3 Results and discussion

3.1 Curve of mechanical strain vs number of cycles to failure

Fig.3 shows the curve of mechanical strain vs number of cycles to failure. During the range of mechanical strain amplitude, the lifetime of OP loading TMF tests was lower than that of IP loading TMF tests.

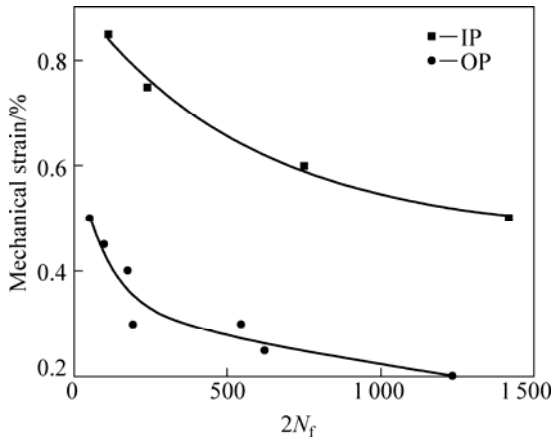

Fig.3 Curve of mechanical strain vs number of cycles to failure

The lifetime of OP loading was close to that of IP loading while mechanical strian amplitude went down and then they had a cross point at the number of cycles to failure of 241 801.

3.2 Cyclic stress response (CSR) behaviors during TMF testing

The stress−strain hysteresis loops at half number of cycles to failure, $N_f/2$, in the different temperature−strain cycles of the IP and OP loading TMF tests with respect to the temperature range of 500−800 °C and mechanical strain amplitude of $\varepsilon_{mech}/2$=0.5% are shown in Fig.4. During TMF tests, the curves of cycling stress response (CSR) showed that IP and OP had a different hardening and softening tendency, and hysteresis loops exhibited two apparent asymmetry: one was zero asymmetry and the other was tensile and compressive asymmetry. OP loading yielded high maximum tensile and low maximum compressive stress and therefore a positive mean stress; while IP loading yielded a lower maximum tensile and a higher maximum compressive stress and therefore a negative mean stress (Fig.4). As to IP loading, the strain imposed on the sample reached the maximum when temperature got to the highest, i.e. 800 °C, and the minimum strain was corresponding to the lowest temperature, i.e. 500 °C. On the contrary, with respect to OP loading, the minimum strain is corresponding to the highest temperature and the maximum strain corresponding to the lowest temperature.

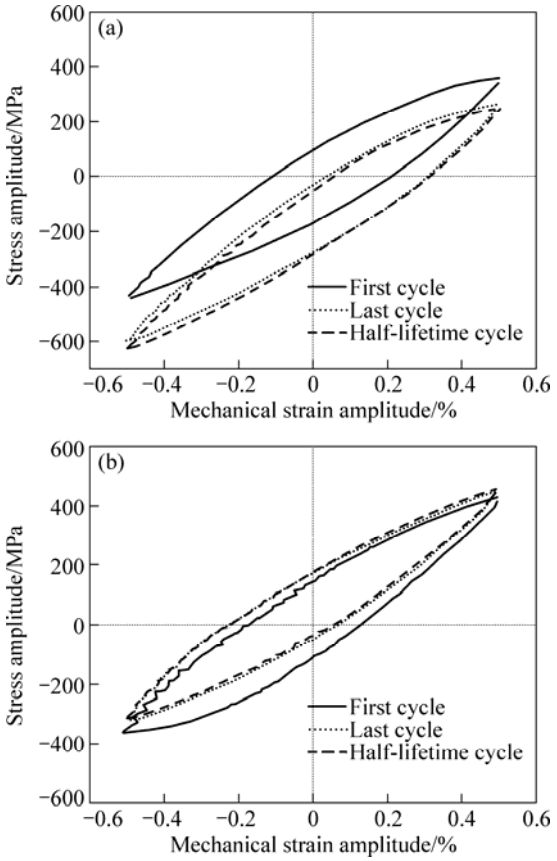

Fig.4 Hysteresis loops of thermo-mechanical fatigue with $\Delta\varepsilon_{mech}/2$=0.5%: (a) IP; (b) OP

The flow stresses of materials were reduced with the increase of temperature, thus thermal activation of atom cut down the ability for material's resistance to deformation, so that the stress needed for the same strain would be lower than that at lower temperature. Therefore, tensile stress at higher temperature was lower than compressive stress at lower temperature as to IP loading at the same strain amplitude, and compressive stress at higher temperature was lower than tensile stress at lower temperature. The sample was applied a compressive mean stress during IP-TMF tests while a tensile mean stress during OP-TMF tests. So, saturation stress at half cycle to failure for IP loading was smaller than that for OP loading with the same strain amplitude during tensile peak stress cycle, and it reversely occurred during compressive peak stress cycle. Totally, stress peak corresponding to lower temperature was higher than that corresponding to higher temperature during both IP loading and OP loading, as evidently found in Fig.4.

There are many factors that affect CSR behavior of gamma-TiAl alloy. The factors for asymmetry of CSR curves during TMF testing are material constants, such as elastic modulus (E), shear modulus (G) and Poisson ratio (μ) which are obviously affected by temperature. E and G have a slightly drop and μ has a slightly lift with

temperature increasing. Strain amplitudes and phases also play an important role which cannot be separated from deformation microstructure during TMF testing.

Furthermore, the stress−strain curves opened widely when being applied with higher strain amplitude, while became snarrow with rising the strain amplitude during both IP loading and OP loading. Hysteresis loops at half number of cycles to failure were very close to the loop at last cycle, which showed that hardening and softening obtained a cyclic saturation when TMF testing proceeded to a half number of cycles to failure as to both IP loading and OP loading.

Gamma-TiAl alloys usually have a notable hardening or softening when being applied with alternating stress at elavated temperature, so study on cyclic stress respondence behaviors of gamma-TiAl should be particularly necessary for their applications as high-temperature structural parts. The curves of cyclic stress response of TiAl alloy for TMF tests under IP loading and OP loading are shown in Fig.5. Under IP loading, stress at first evidently had a fast softening, then gradually saturated and at last continuously softened till fracture in tensile peak stress cycle; while stress at first had a fast hardening, then gradually saturated and at last continuously hardened till fracture in compressive peak stress cycle. On the contrary, under OP loading, stress at first had a fast hardening, then gradually saturated followed by continuous hardening till fracture in tensile peak stress cycle, while stress at first had a fast softening, then gradually saturated followed by continuous softening till fracture in compressive peak stress cycle. During the whole cycle, an apparent difference was that the time needed for hardening or softening under OP loading was shorter than that under IP loading, and with reducing the mechanical strain amplitude, stress would be saturated after a number of 100 cycles under OP loading.

3.3 Configuration of dislocations, slips and twins during TMF

During IP loading TMF tests, a large number of line dislocations and spot dislocations and little twins distributed in gamma-TiAl alloy at higher strain amplitudes, which showed that slip modes mainly were cross slip and climb slip, as seen in Fig.6.

During tensile peak stress cycle, more and more slip systems would be activated on the favorable orientation of the (α_2/γ) interface, then these new slip systems crossed along the two sides of lamellae if the peak stress in alloy was rather high so as to reach the critical shear stress and dislocations would tangle when two dislocations originated from phase interface spread

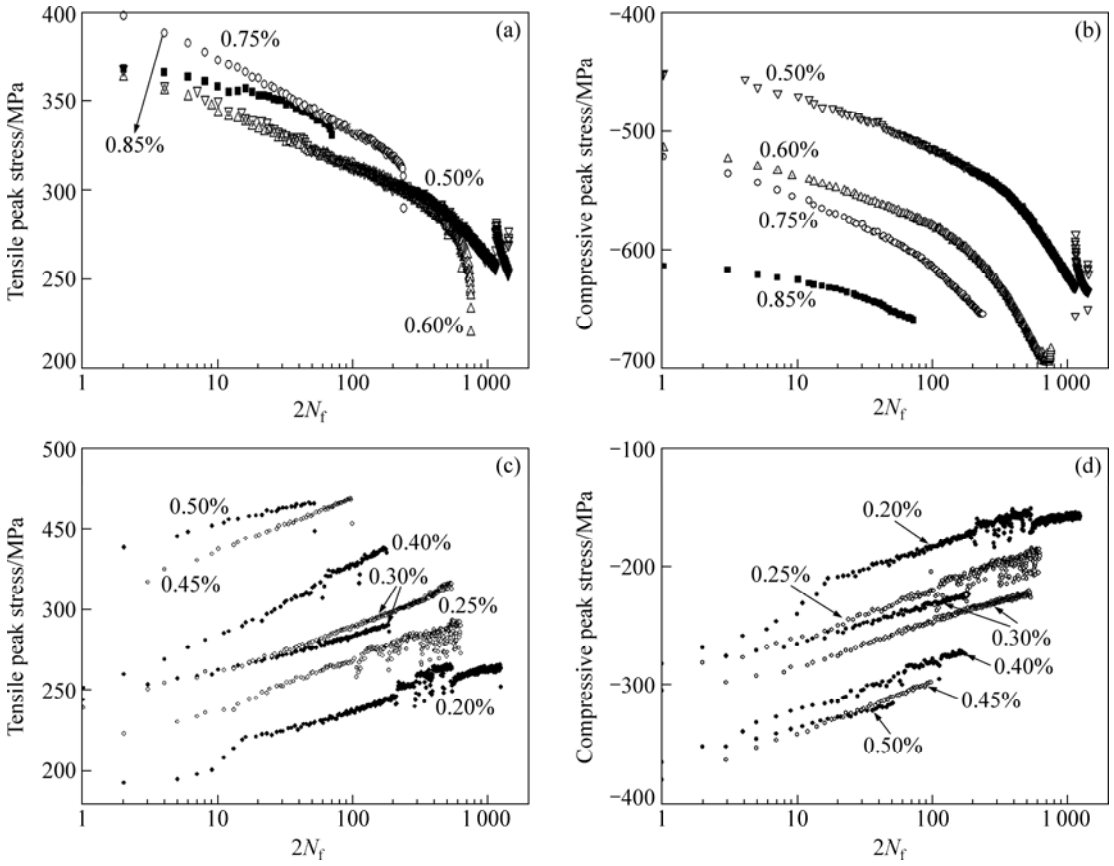

Fig.5 Cyclic stress response curves of thermo-mechanical fatigue tests: (a) IP in tensile peak stress cycle; (b) IP in compressive peak stress cycle; (c) OP in tensile peak stress cycle; (d) OP in compressive peak stress cycle

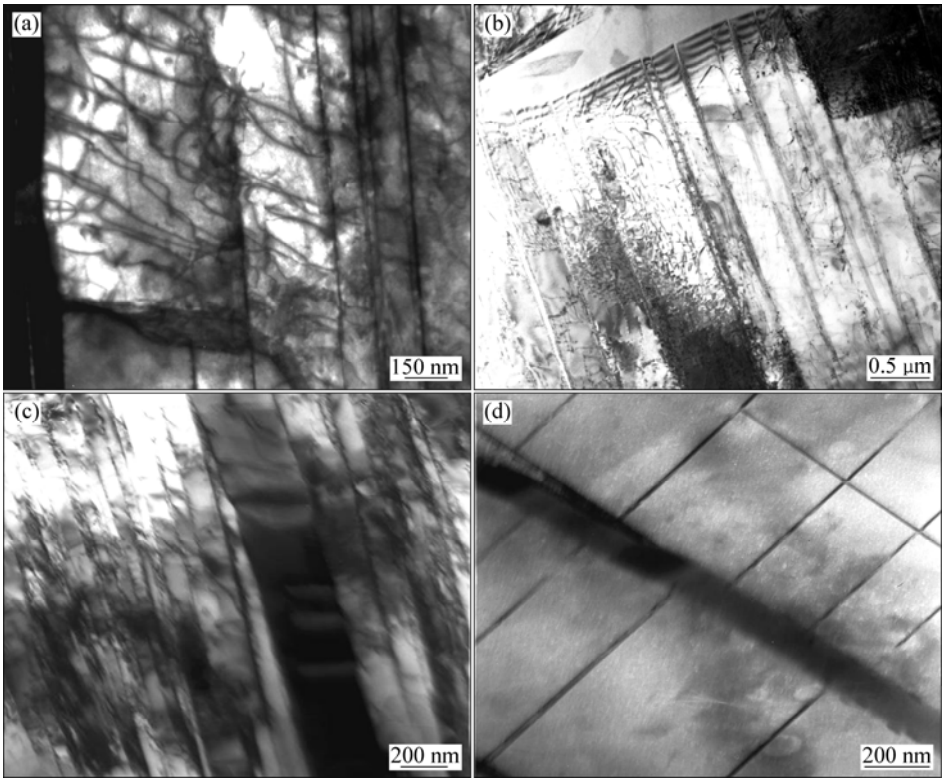

Fig.6 Dislocation configuration and slip modes during IP-TMF testing: (a) and (b) IP, $\Delta\varepsilon_{mech}/2$=0.75%; (c) and (d) IP, $\Delta\varepsilon_{mech}/2$=0.5%

through the lamellar and met together. Dislocation climbing usually took place when the temperature rose above 700 °C[19]. The competetion of dislocation tangles, dislocation loops annihilation and dislocation loops coarsening would contribute to the cyclic softening above 700 °C. Meanwhile, flow stress decreased with the increase of temperature, thus weakening some slip bands, and movable dislocations could pass through phase interface of α_2/γ and cut off α_2 lamella, therefore fast softening at first cycles was found during first cycles on the curve of cyclic stress response. During compressive peak stress cycle, flow stress increased with the decrease of temperature, thus bonding strength of phase interfaces would be a little improved so that these actuated slip systems and movable dislocation cannot move and piled up ahead the phase interfaces and boundaries. Furthermore, deformation capability of TiAl alloy would decline below 650 °C which is in the ductile-brittle transition range, and dislocations piled up severely ahead the phase interfaces and boundaries. Softening in tensile peak stress cycles and hardening in compressive peak stress cycles would last for several cycles, which indicated the continuity of CSR.

During TMF tests by IP loading, slip mode transformed from cross-slip and climbing to single planar slip, which was decided by peak stress when strain amplitude was reduced to 0.5%. Falling off of peak stress arose from the drop of strain amplitude and thus dislocation would no longer originate from phase interfaces of α_2/γ and boundaries when peak stress was reduced to below critical shear stress. In tensile peak stress cycle, dislocation maybe occured at preferred orientation since slow stress was evidently decreased and the corresponding deformation ability was strengthened at elavated temperature. Therefore, some slip systems which lay in soft orientation would extend, but only little slip systems could work and few dislocations mainly slipped with a planar mode which was affected by peak stress. Some small spot-dislocations and dislocation lines could be found within lamellar, which revealed that cross slip and climbing also existed during TMF testing. Meanwhile, some deformation twins were found, as illustrated in Fig.6(d). Those deformation twins certainly were contributed to plastic deformation. On the other hand, the formation of deformation twins could change the orientation of crystal, thus making hard orientation shift to easy orientation, and dislocations located in this region could move again so that plastic deformation could last continuously.

Similiarly, a large number of dislocation lines and spot dislocations could be found in TiAl alloy after TMF tests by OP loading at higher strain amplitude, but little twins, stacking fault and multiple slip existed, which indicated that slip modes mainly were cross-slip and climbing, as shown in Fig.7. A large spot dislocations and some short dislocation lines oriented within lamellae

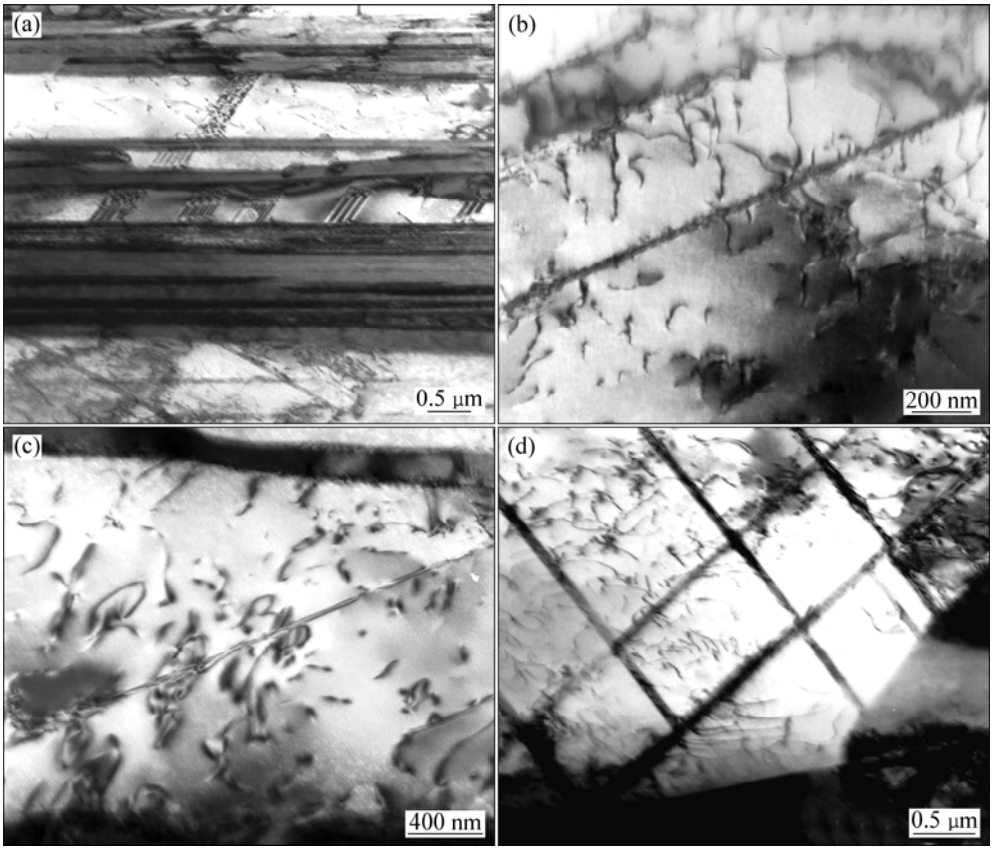

Fig.7 Dislocation configuration and slip modes during OP-TMF testing with $\Delta\varepsilon_{mech}/2$ of 0.5%: (a) Stacking fault, twins and multiple slip distributing along interfaces of α_2/γ and within γ lamellae; (b) and (c) Large number of dislocation lines located at wider γ lamellae; (d) Cross slip bands and climbing bands distributing within wider γ lamellae

and numerous stacking faults distributed along the interfaces of α_2/γ and boundaries companied with deformation twins formed when strain amplitude was reduced.

When temperature went down from 650 °C to 500 °C, flow stress persisted in enhancing so that stress was high enough to approach to the value needed for considerable plastic deformation. As a result, at the first step during tensile peak stress half cycle by OP loading, dislocation quantity and density gradually increased under rather lower temperature and dislocation were restricted to move among several planar slip bands so that work hardening lastly aggravated. Planar slip was no longer the dominant mode in activation of multiple slip systems and evenly distributed dislocations would cut off α_2 particles or α_2 lamellae, then dislocations reaction appeared followed by nucleation of γ phase and resistance to dislocations movement would be weaker which called friction stress softening[4].

Furthermore, dislocations disappeared on the main slip plane during cross slip and climb, therefore dislocations located at different slip bands or adjacent slip planes would annihilate or reorganize, which made adjacent slip bands merge into rather wide slip bands, as shown in Fig.7(d), so that deformation usually took place within wide slip bands that produced little obstacle to plastic deformation, leading to continuous softening above 650 °C.

4 Conclusions

1) During TMF tests by IP loading, CSR had a significant softening during tensile peak stress cycle and an apparent hardening during compressive peak stress cycle; while a significant hardening during tensile peak stress cycle and an apparent softening during compressive peak stress cycle appeared with respect to OP loading.

2) On the hysteresis loops two apparent asymmetries appeared. One was zero asymmetry and the other was tensile and compressive asymmetry, which yielded a negative mean stress by IP loading and a positive mean stress by OP loading.

3) During TMF tests by IP loading, slip mode transformed from cross-slip and climbing to single planar slip with the decrese of strain amplitude affected by peak stress.

4) During TMF tests by OP loading, a large nuber

of dislocations and a little twins, stacking fault and multiple slip bands could be found at higher strain amplitude.

5) Dislocations configuration and slip behaviors were contributed to cyclic hardening or cyclic softening.

References

[1] KIM Y W. Strength and ductility in TiAl alloys [J]. Intermetallics, 1998, 6(7/8): 623−628.

[2] LIU C T, KIM Y W. Room-temperature environmental embrittlement in a TiAl alloy [J]. Scripta Metallurgica et Materialia, 1992, 27(5): 599−603.

[3] HUANG J S, KIM Y W. Creep deformation and fracture of a two-phase TiAl alloy [J]. Scripta Metallurgica et Materialia, 1991, 25(8): 1901−1906.

[4] LEYENS C, PETERS M. Titanium and titanium alloys [M]. CHEN Zhen-hua, transl. Beijing: Chemical Industry Press, 2005: 94−99.

[5] ZHANG Cheng-jun, FU Heng-zhi, XU Da-ming, GUO Jing-jie, BI Wei-sheng, SU Yan-qing. Feasibility of integrated seed making and directional solidification of TiAl alloy using cold crucible [J]. Transactions of Nonferrous Metals Society of China, 2009, 19(2): 330−334.

[6] DU X W, ZHU JING, ZHANG X, CHENG Z Y, KIM Y W. Creep induced $\alpha_2 \rightarrow \beta_2$ phase transformation in a fully-lamellar TiAl alloy [J]. Scripta Materialia, 2000, 43(7): 597−602.

[7] YOSHIHARA M, KIM Y W. Oxidation behavior of gamma alloys designed for high temperature applications [J]. Intermetallics, 2005, 13(9): 952−958.

[8] XIAO Dai-hong, HUANG Bai-yun. Superplastic behavior and microstructure evolution of as-cast Ti-47Al-8Cr -2Nb alloy at lower temperature [J]. The Chinese Journal of Nonferrous Metals, 2008, 18(10): 1749−1756. (in Chinese)

[9] ZHUANG Jun-hong, HUANG Bai-yun, HE Yue-hui, MENG Li-ping. Mechanical behaviors of TiAl alloy during low temperature superplastic deformation [J]. The Chinese Journal of Nonferrous Metals, 2003, 13(2): 442−446. (in Chinese)

[10] MALAKONDAIAH G, KIM Y W, NICHOLAS T. Some observations on the ambient temperature deformation behavior of fully lamellar Ti-46Al-2Nb-2Cr alloy [J]. Scripta Metallurgica et Materialia, 1994, 30(7): 939−944.

[11] ROTH M, BIERMANN H. Thermo-mechanical fatigue behaviour of the γ-TiAl alloy TNB-V5 [J]. Scripta Materialia, 2006, 54: 137−141.

[12] CHRIST H J, FISCHER F O R, MAIER H J. High-temperature fatiuge behavior of a near-γ titanium aluminide alloy under isothermal and thermomechanical conditions [J]. Materials Science and Engineering A, 2001, 319/320/321: 625−630.

[13] MALKONDAIAH G, NICHOLAS T. High-temperature low-cycle fatigue of a gamma titanium aluminide Ti-46Al-2Nb-2Cr [J]. Metallurgical and Materials Transactions A, 1996, 27(8): 2239−2251.

[14] XIANG Hong-fu, GAO Qiang, CUI Yu-you, LI Shou-xin, YANG Rui. Study on thermo-mechanical fatigue of Ti-46.5Al-5Nb alloy [J]. Acta Metallurgica Sinica, 2002, 38: 451−453. (in Chinese)

[15] XIANG Hong-fu. Study of fatigue behavior and deformation mechanisms of γ-TiAl alloys [D]. Shenyang: Institue of Metal Research, Chinese academy of Sciences, 2006: 25−78. (in Chinese)

[16] BAUER V, CHRIST H J. Thermomechanical fatigue behaviour of a third generation γ-TiAl intermetallic alloy [J]. Intermetallics, 2009, 17(5): 370−377.

[17] ROTH M, BIERMANN H. Thermo-mechanical fatigue behaviour of a modern γ-TiAl alloy [J]. International Journal of Fatigue, 2008, 30(2): 352−356.

[18] CUI W F , LIU C M, BAUER V, CHRIST H J. Thermomechanical fatigue behaviours of a third generation γ-TiAl based alloy [J]. Intermetallics, 2007, 15(5/6): 675−678.

[19] BERANGER A S , FEAUGAS X, CLAVEL M. Low cycle fatigue behavior of an $\alpha+\beta$ titanium alloy: Ti6246 [J]. Materials Science and Engineering A, 1993, 172(1/2): 31−41.

(Edited by YANG Bing)